AXIAL FEEDBACK STABILIZATION OF FLUTE MODES FOR MIRROR MACHINES

by

B.K. Kang, M.A. Lieberman, and A.K. Sen

Memorandum No. UCB/ERL M84/61

3 August 1984

ELECTRONICS RESEARCH LABORATORY

College of Engineering
University of California, Berkeley, CA 94720

AXIAL FEEDBACK STABILIZATION OF FLUTE MODES FOR MIRROR MACHINES

B. K. Kang, M. A. Lieberman, and A. K. Sen

Electronics Research Laboratory
University of California, Berkeley, CA 94720

The possibility of feedback stabilization of the $m = 1$ MHD flute mode for axisymmetric mirror machines is examined. By a proper choice of feedback function, the $m = 1$ flute mode on the core plasma is stabilized by feedback signals applied to segmented, ring shaped feedback plates which are in end-contact with the relatively cold external halo plasma. A three region plasma model is developed and analyzed, consisting of a hot core surrounded by a warm transition annulus, which is in turn surrounded by a warm halo annulus that is in contact with the feedback plates at the two endwalls. A simple feedback transfer function is chosen, and root locus plots versus the feedback gain are calculated for plasma parameters characteristic of the MFTF-B device at Lawrence Livermore Laboratory and the MMX device at the University of California, Berkeley. We conclude that feedback stabilization of the $m = 1$ flute mode can be achieved in either device with a modest feedback gain.

I. INTRODUCTION

Research on stabilizing the $m = 1$ MHD flute mode in axisymmetric mirror machines has been persued by several authors using axial feedback[1-5] using radial feedback[6], and modifying the line-tying admittance[7-10]. Radial feedback applies electrostatic signals to feedback plates around the plasma to suppress the flute mode, whereas axial feedback applies the feedback signals to feedback plates located at an end of the machine.

Earlier, an in-depth study[5] on line-tying and feedback stabilization of the flute mode for a simple mirror pointed out that the endwall sheath, which provides the thermal insulation for the hot plasma by reducing electron conduction to the endwall, would strongly degrade the stabilization due to line-tying alone, and concluded that line-tying alone will not stabilize the flute mode in a simple mirror. Lieberman et al[1,2], Wong[3], and Vandegrift[4] have shown that, for low-beta low-temperature mirror machines, the flute mode can be stabilized by applying feedback signals on pie-shaped feedback plates located at the end of the machine.

The U.C. Irvine group showed that flute stability can be obtained by increasing the line-tying admittance. Wickham and Vandegrift[7,8] modified the line-tying admittance by heating an electron emitting end-plate. They observed a reduced flute growth rate, and pointed out that the system becomes flute stable if the end-plate emits enough electrons. Direct heat conduction to an electron-emitting end-plate leads to excessive heat loss from the hot core plasma. It has been suggested that the feedback plate be halo-shaped and in contact with only the relatively cold external plasma. Vandegrift et al[9] used

a halo-shaped electron emitting end-plate to modify the line-tying admittance, observed reduced flute growth rate, and postulated that a larger mirror system may become flute stable if the halo-shaped end-plate's inner radius is extended to the radius where the plasma density, with a profile assumed to be a Gaussian, drops to $1/e$ of the peak density. However, the end-wall heat loss is still too great at the radius where the density drops by $1/e$.

Here, we explore the possibility of stabilizing the flute unstable system by applying proper feedback signals on halo-shaped feedback plates with arbitrary inner and outer radii located at the end of the machine. In section *II*, we represent the mirror confined plasma system with a three layer model and obtain the dispersion relation and feedback equation for the system. In section *III*, we apply our feedback equation to the MFTF-B experiment and the Berkeley 10 meter Multiple Mirror Experiment (MMX). In section *IV*, we discuss the results and limitations of our three layer model.

II. FEEDBACK MODEL AND EQUATION

Fig.1 shows the three layer model for the mirror confined plasma which we consider here. Regions *I* -*IV* represent the core plasma, the transition plasma, the external halo plasma, and the surrounding vacuum region, respectively. The transition plasma (region *II*) couples the core plasma (region *I*) to the halo plasma (region *III*), on which the feedback signal is applied axially through segmented, halo-shaped feedback plates located at the end of the machine.

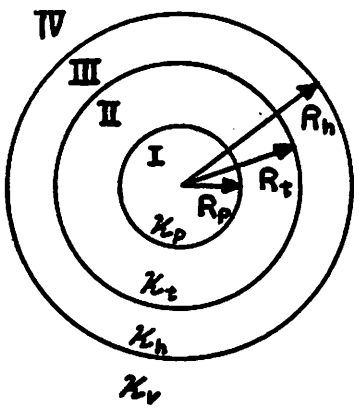

Fig.1
Three layer model for
the mirror confined plasma.

For the $m = 1$ flute mode, in cylindrical coordinates, we represent the perturbed potential ϕ which vanishes at $r = \infty$ as

$$\begin{aligned}
\phi_p &= Ar\cos\theta, \\
\phi_t &= Br\cos\theta + \frac{C}{r}\cos\theta, \\
\phi_h &= Dr\cos\theta + \frac{E}{r}\cos\theta, \\
\phi_v &= \frac{F}{r}\cos\theta.
\end{aligned} \tag{1}$$

Enforcing the boundary conditions on (1), i.e., that ϕ and the normal component of the electric displacement $\mathbf{D}$ be continuous across the boundary, and assuming that the dielectric constants for the plasma are much greater than the vacuum ($\kappa_p, \kappa_t, \kappa_h \gg 1$) we obtain the dispersion relation as

$$\begin{aligned}
&(\kappa_p + \kappa_t)(\kappa_t - \kappa_h)\frac{1}{R_p^2 R_h^2} - (\kappa_t - \kappa_p)(\kappa_t + \kappa_h)\frac{1}{R_t^2 R_h^2} \\
&+(\kappa_p + \kappa_t)(\kappa_t + \kappa_h)\frac{1}{R_t^2 R_p^2} + (\kappa_t - \kappa_p)(\kappa_t - \kappa_h)\frac{1}{R_t^4} = 0
\end{aligned} \tag{2}$$

where, R_p, R_t, and R_h are the radii of the core, transition, and halo boundaries, respectively.

We use the dielectric constants derived by Lieberman and Wong[1,2] for a gravitationally driven, $m = 1$ flute mode, in a magnetically confined plasma that is connected to a conducting endwall through a sheath having admittance per unit area y_α, under the assumptions that the curvature and the electric drift effect dominate over the ∇B and the diamagnetic drift effect (cold, low-beta,weak ∇n_o plasma in the slab geometry):

$$\kappa = 1 + \sum_\alpha \frac{\omega_{p\alpha}^2}{\Omega_\alpha^2} - \sum_\alpha \frac{1}{\omega + \omega_\alpha}\left(\frac{1}{kR_p}\frac{\omega_{p\alpha}^2}{\Omega_\alpha} + j\frac{y_\alpha}{\epsilon_o k^2 l_T}\right) \tag{3}$$

where, $\omega_{p\alpha}^2 = q_\alpha^2 n_\alpha/(\epsilon_o m_\alpha)$, $\Omega_\alpha = q_\alpha B/m_\alpha$, $\omega_\alpha = k g_\alpha/\Omega_\alpha$, $g_\alpha = v_{th\alpha}^2/R_c$, R_c is the field line radius of curvature, l_T is the total plasma length, $v_{th\alpha}$ is the root mean square thermal velocity for the species α, and $k = m/r$ is the wave number for a perturbation of the form $e^{j(\omega t - m\theta)}$.

Since, $\omega_{pi}^2/\Omega_i^2 \gg 1$, $\omega_{pi}^2\Omega_e^2/(\omega_{pe}^2\Omega_i^2) = m_i/m_e \gg 1$, and assuming that the core temperature is much higher than the transition or halo temperature, we can write

$$\kappa_p \approx \frac{\omega_{pi}^{I^2}}{\Omega_i^2} - \frac{1}{\omega + \omega_i}\frac{\omega_{pi}^{I^2}}{\Omega_i} - \frac{1}{\omega + \omega_e}\frac{\omega_{pe}^{I^2}}{\Omega_e}, \tag{4}$$

$$\kappa_t \approx \frac{\omega_{pi}^{II^2}}{\Omega_i^2}, \tag{5}$$

$$\kappa_h \approx \frac{\omega_{pi}^{III^2}}{\Omega_i^2} - \frac{1}{\omega}\left(j\frac{y_e}{\epsilon_o k^2 l_p}\right). \tag{6}$$

A typical tandem mirror geometry is shown in Fig.2. The bad curvature drive is concentrated mainly in the plug regions having characteristic length l_p.

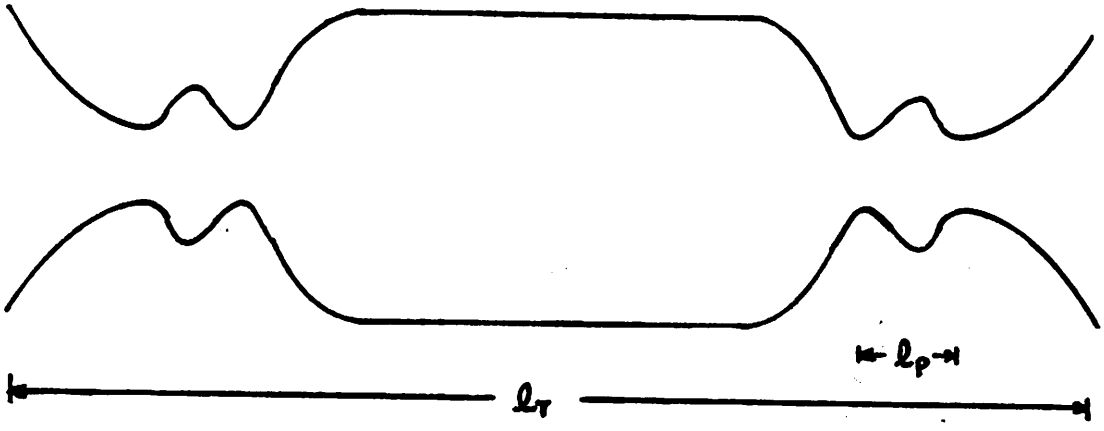

Fig.2 A typical tandem mirror geometry.

We define $\epsilon_i \equiv a_i^2 l_p/(l_B^2 l_T)$, $\epsilon_e \equiv a_e^2 l_p/(l_B^2 l_T)$, $\bar{\epsilon} \equiv (\epsilon_i + \epsilon_e)/2$, and $u \equiv (\omega - \Omega_i \epsilon_i)/\Omega_i$. Here, a_α is the mean gyroradius for the species α, l_B is the mirror scale length of the plug, and u is the doppler shifted frequency normalized to the ion gyrofrequency Ω_i. Note that $\bar{\epsilon}^{1/2}$ is a normalized characteristic MHD growth rate;

$$\bar{\epsilon}^{1/2} = \left(\frac{g/R_p}{\Omega_i^2}\right)^{1/2} = \frac{\gamma_{mhd}}{\Omega_i}.$$

We rewrite (4) and (6) as

$$\kappa_p = \frac{\omega_{pi}^{I^2}}{\Omega_i^2} - \left(\frac{1}{u} - \frac{1}{u - 2\bar{\epsilon}}\right)\frac{1}{\Omega_i}\frac{en}{\epsilon_o B}, \tag{4'}$$

$$\kappa_h = \frac{\omega_{pi}^{II^2}}{\Omega_i^2} + \frac{1}{j\Omega_i(u - \epsilon_i)}\frac{y_e}{\epsilon_o k^2 l_p}. \tag{6'}$$

Multiplying (4'), (5), and (6') by

$$-\epsilon_o k^2 A_p l_T (u - 2\bar{\epsilon}) u \frac{\Omega_i^2}{j\omega},$$

we have, respectively,

$$-\epsilon_o \kappa_p k^2 A_p l_T (u - 2\bar{\epsilon}) u \frac{\Omega_i^2}{j\omega} = j\omega C_p + Y_{p\phi} + \frac{1}{j\omega L_p} \equiv Y_p, \tag{7}$$

$$-\epsilon_o \kappa_t k^2 A_t l_T (u - 2\bar{\epsilon}) u \frac{\Omega_i^2}{j\omega} \frac{A_p}{A_t} = (j\omega C_t + Y_{t\phi}) \frac{A_p}{A_t} \equiv Y_t \frac{A_p}{A_t}, \tag{8}$$

$$-\epsilon_o \kappa_h k^2 A_h l_T (u - 2\bar{\epsilon}) u \frac{\Omega_i^2}{j\omega} \frac{A_p}{A_h} = (j\omega C_h + Y_{h\phi} + Y_{he}) \frac{A_p}{A_h} \equiv Y_h \frac{A_p}{A_h}, \tag{9}$$

where, Y_p, Y_t, and Y_h are the effective admittance of the core, transition, and halo plasmas, respectively,

$$C_p = \frac{\epsilon_o k^2 A_p l_T \omega_{pi}^{I^2}}{\Omega_i^2}, \qquad Y_{p\phi} = -j \frac{2\epsilon_o k^2 A_p l_T \bar{\epsilon}_p \omega_{pi}^{I^2}}{\Omega_i},$$

$$L_p^{-1} = -2\epsilon_o k^2 A_p l_T \omega_{pi}^{I^2} \bar{\epsilon}_p, \qquad C_t = \frac{\epsilon_o k^2 A_t l_T \omega_{pi}^{II^2}}{\Omega_i^2},$$

$$Y_{t\phi} = -j \frac{2\epsilon_o k^2 A_t l_T \bar{\epsilon}_t \omega_{pi}^{II^2}}{\Omega_i}, \qquad C_h = \frac{\epsilon_o k^2 A_h l_T \omega_{pi}^{III^2}}{\Omega_i^2},$$

$$Y_{h\phi} = -j \frac{2\epsilon_o k^2 A_h l_T \bar{\epsilon}_h \omega_{pi}^{III^2}}{\Omega_i}, \quad \textit{and} \quad Y_{he} = y_e A_h.$$

The physical meaning of each of these elements is explained in Wong[3] and Vandegrift[4]. Briefly, the $C's$ are the capacitances seen across the flute surfaces, $L_p < 0$ is the inductance driving the flute mode, and the Y_ϕ's represent the stabilising effect on the flute mode due to the finite rotational frequency (see Appendix for futher details). By putting (7), (8), and (9) into (2) multiplied by

$$\frac{1}{\pi^4} \left(\epsilon_o k^2 A_p l_T (u - 2\bar{\epsilon}) u \frac{\Omega_i^2}{j\omega}\right)^2,$$

we can rewrite the dispersion relation without feedback in terms of the circuit elements as

$$Y_p Y_h + Y_t Y_h \frac{R_p^2}{(R_t^2 - R_p^2)^2} (R_p^2 + R_t^2) + Y_t^2 \frac{R_p^2 (R_h^2 + R_t^2)}{(R_t^2 - R_p^2)^2}$$
$$+ Y_p Y_t \frac{(R_t^2 + R_h^2)(R_t^2 + R_p^2)}{(R_t^2 - R_p^2)^2} = 0. \tag{10}$$

Now, we consider the equivalent circuit representation Fig.3.

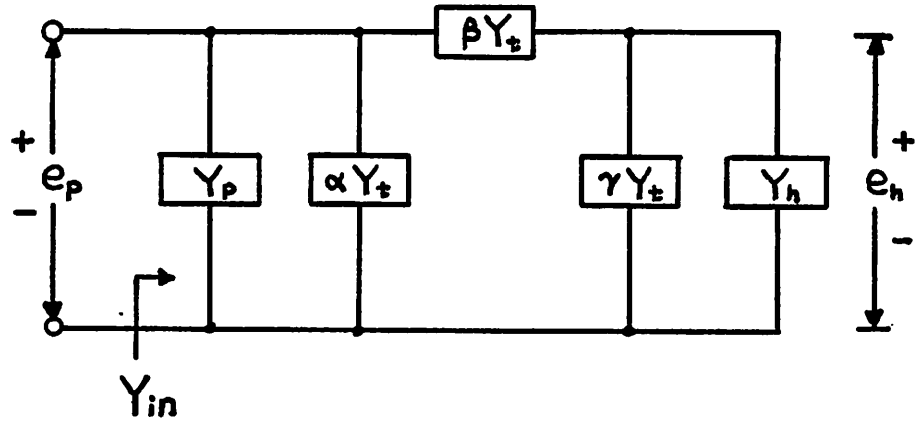

Fig.3 Circuit representation of three layer model without feedback.

Taking $Y_{in} = 0$ (resonance), we obtain

$$Y_p Y_h + (\alpha+\beta) Y_t Y_h + (\alpha\beta + \beta\gamma + \alpha\gamma) Y_t^2 + (\beta+\gamma) Y_t Y_p = 0. \qquad (11)$$

By comparing (10) with (11), we can recover the dispersion relation by setting

$$\alpha + \beta = \frac{R_p^2 (R_p^2 + R_t^2)}{(R_t^2 - R_p^2)^2}, \qquad (12)$$

$$\beta + \gamma = \frac{(R_t^2 + R_h^2)(R_t^2 + R_p^2)}{(R_t^2 - R_p^2)^2}, \qquad (13)$$

$$\alpha\beta + \beta\gamma + \alpha\gamma = \frac{R_p^2 (R_h^2 + R_t^2)}{(R_t^2 - R_p^2)^2}. \qquad (14)$$

Solving for α, β, γ, we obtain

$$\alpha = \frac{R_p^2 (R_p^2 + R_t^2)}{(R_t^2 - R_p^2)^2} - \beta \qquad (15)$$

$$\beta = \frac{2 R_p^2 R_t (R_t^2 + R_h^2)^{1/2}}{(R_t^2 - R_p^2)^2} \qquad (16)$$

$$\gamma = \frac{(R_t^2 + R_h^2)(R_t^2 + R_p^2)}{(R_t^2 - R_p^2)^2} - \beta \qquad (17)$$

(For typical parameters of MFTF-B, $\alpha \sim -3$, $\beta \sim 5$, $\gamma \sim 8$) . The form of these coupling coefficients α, β, γ for MFTF-B imply the following: *i*) The effective capacitance of the core plasma is decreased compared to the capacitance due to the core plasma alone, because charge cancellation occurs at the boundary with the transition plasma. *ii*) If the halo plasma is perfectly line-tied, i.e., $Y_{he} \rightarrow \infty$, the effective capacitance due to the transition and halo plasma is about $2C_t < C_p$. Thus, the growth rate of the flute instability is somewhat reduced due to the increased inertia of the system, but there is no circuit element which provides $L > 0$ that can compensate $L_p < 0$ to obtain complete stability. *iii*) If we provide a positive inductance by feedback, we might have stability.

Now, we consider an equivalent circuit model with feedback. With feedback voltage applied at the halo shaped feedback plates located at the end of the machine, the lower terminal of the line-tying admittance is forced away from system ground. So, we can represent the equivalent circuit model of the system as Fig.4, where $Y_1 \equiv Y_h - Y_{he}$.

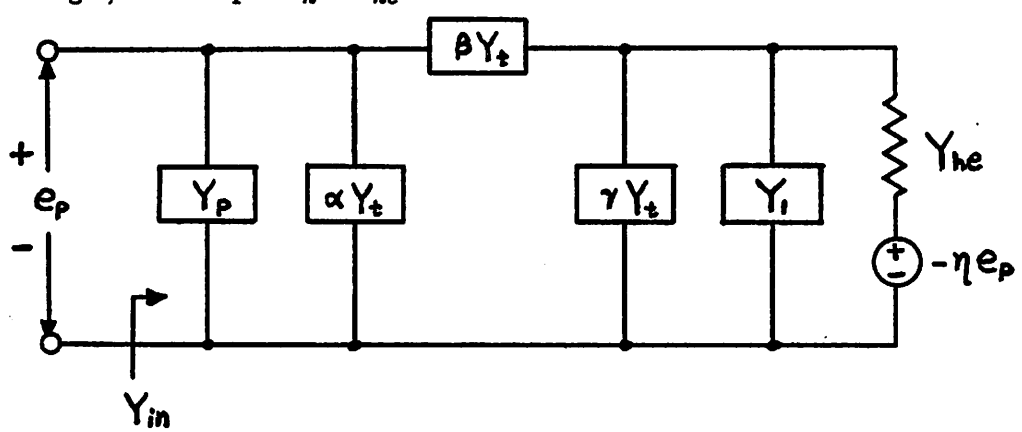

Fig.4 Circuit representation of three layer model with feedback.

By taking $Y_{in} = 0$, we obtain the dispersion relation with feedback:

$$Y_p + \alpha Y_t + \frac{\beta Y_t(\gamma Y_t + Y_h)}{(\beta+\gamma)Y_t + Y_h} + \frac{\beta Y_t \eta Y_{he}}{(\beta+\gamma)Y_t + Y_h} = 0 \qquad (18)$$

where, η is the voltage transfer function of the feedback network. A simple schematic feedback diagram is shown in Fig.5.

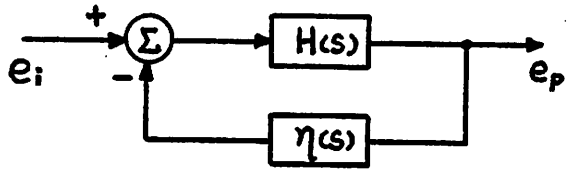

Fig.5 Schematic representation of the system with feedback ($e_i = 0$ corresponds to Fig.4).

We can analyze this problem with more general feedback theory, but for simplicity, we consider the case $e_i = 0$ ($e_i \neq 0$ corresponds to a signal that may be mixed with the feedback signal to obtain overall stability of the system). If we choose the feedback transfer function $\eta(s)$ as

$$\eta(s) = -\frac{G}{sL_p}\frac{(\beta+\gamma)Y_t + Y_h}{\beta Y_t Y_{he}}, \qquad (19)$$

the negative inductance included in Y_p cancels out from (18) for $G = 1$, and the system becomes stable. However, the feedback function $\eta(s)$ given by (19) is practically difficult to construct, because Y_t and Y_h contain imaginary conductance terms (the Y_ϕ's). So, we delete all Y_ϕ's in the feedback function (19), and examine the system stability with the easily realizable feedback function:

$$\eta(s) = -\frac{G}{sL_p}\frac{(\beta+\gamma)sC_t + sC_h + Y_{he}}{\beta s C_t Y_{he}}. \qquad (20)$$

The numerator of (18) with $\eta(s)$ given by (20) becomes

$$
\begin{aligned}
&s^4\left((C_p+\alpha C_t)(C_h+(\beta+\gamma)C_t)+\beta C_t(C_h+\gamma C_t)\right)\\
&+s^3\Big((C_h+(\beta+\gamma)C_t)(Y_{p\phi}+\alpha Y_{t\phi})+(C_p+\alpha C_t)(Y_{h\phi}+Y_{he}+(\beta+\gamma)Y_{t\phi})\\
&\qquad+\beta Y_{t\phi}(C_h+\gamma C_t)+\beta C_t(Y_{h\phi}+Y_{he}+\gamma Y_{t\phi})\Big)\\
&+s^2\Big(L_p^{-1}(C_h+(\beta+\gamma)C_t)+(Y_{p\phi}+\alpha Y_{t\phi})(Y_{h\phi}+Y_{he}+(\beta+\gamma)Y_{t\phi})\\
&\qquad+\beta Y_{t\phi}(Y_{h\phi}+Y_{he}+\gamma Y_{t\phi})-GL_p^{-1}(C_h+(\beta+\gamma)C_t)\Big)\\
&+s\left(L_p^{-1}(Y_{h\phi}+Y_{he}+(\beta+\gamma)Y_{t\phi})-\frac{G}{L_pC_t}(C_tY_{he}+Y_{t\phi}(C_h+(\beta+\gamma)C_t)\right)\\
&-\frac{G}{L_pC_t}Y_{t\phi}Y_{he}=0
\end{aligned}
\tag{21}
$$

where, $s=j\omega$ and G is a constant feedback gain. If we neglect all the Y_ϕ's, i.e., finite rotational frequency effects, we have

$$
\begin{aligned}
&s^4\left((C_p+\alpha C_t)(C_h+(\beta+\gamma)C_t)+\beta C_t(C_h+\gamma C_t)\right)\\
&+s^3\left((C_p+\alpha C_t)Y_{he}+\beta C_tY_{he}\right)\\
&+s^2\left(L_p^{-1}(C_h+(\beta+\gamma)C_t)-GL_p^{-1}(C_h+(\beta+\gamma)C_t)\right)\\
&+s\left(L_p^{-1}Y_{he}-GL_p^{-1}Y_{he}\right)=0
\end{aligned}
\tag{22}
$$

If we neglect $Y_{h\phi}$ and $Y_{t\phi}$, which are typically small, but retain $Y_{p\phi}$, and apply azimuthally rotating feedback signals with the rotation frequency the same as the $\mathbf{g}_o\times\mathbf{B}_o$ rotation frequency of the core plasma, then the effect of $Y_{p\phi}$ drops out, and we recover (22) from (21). The zeros of (18) determine the system stability. However, in order to observe a pole-zero cancellation, we write the denominator of (18) explicitly;

$$denom. = s^2\beta L_p C_t Y_{he}\big((\beta+\gamma)(sC_t + Y_{t\phi}) + sC_h + Y_{h\phi} + Y_{he}\big). \qquad (23)$$

We will see in the next section that, by a proper choice of G, the feedback function (20) stabilizes the system.

III. THE RESULTS OF FEEDBACK.

In this section, we apply the results of the previous section for parameters and geometry characteristic of the MFTF-B and the MMX experiments. We discuss the effects of feedback on the system's stability.

A. MFTF-B Experiment

We take the MFTF-B parameters to be as follows;

$$l_B = 1m, \quad l_p = 5m, \quad l_T = 12.8m, \quad R_p = 30cm,$$
$$R_t = 45cm, \quad R_h = 60cm, \quad n_h/n_p = 10^{-1}, \quad n_t/n_p = 10^{-1},$$
$$n_p = 10^{20}m^{-3}, \quad T_p = 10kev, \quad T_h = 50ev, \quad T_t = 50ev,$$

where n_p is the plasma density of the core region. The corresponding circuit elements can be calculated using the above parameters:

* Capacitors

$$C_j = \frac{\epsilon_o k^2 A_p l_T \omega_{pi}^{j^2}}{\Omega_i} = 5.259 \times 10^{-27}\frac{n_j l_T}{B^2}\frac{A_j}{A_p}, \qquad (j = p, t, h)$$
$$C_p = 6.73 \times 10^{-6}[F],$$
$$C_t = 8.43 \times 10^{-7}[F],$$
$$C_h = 1.18 \times 10^{-6}[F].$$

(Note that for the $m = 1$ flute mode, $Ak^2 = \pi$).

* Inductor

$$L_p^{-1} = -2\epsilon_o k^2 A_p l_T \omega_{pi}^{I^2} \bar{\epsilon}_p = -9.644 \times 10^{-11} \bar{\epsilon}_p n_o l_T,$$
$$L_p = -1.03 \times 10^{-7}[H].$$

* Frequency-independent part of the imaginary conductance (Y_ϕ's)

$$Y_{j\phi} = -j9.644 \times 10^{-11} \frac{\bar{\epsilon}_j n_o l_T}{\Omega_i} \frac{A_j}{A_p},$$
$$Y_{p\phi} = -j9.62 \times 10^{-2}[mho],$$
$$Y_{t\phi} = -j4.95 \times 10^{-5}[mho],$$
$$Y_{h\phi} = -j3.52 \times 10^{-5}[mho].$$

* Line - tying admittance

$$Y_{he} = g_{sh} A_h = \frac{1}{4} \frac{\epsilon_o v_i}{\lambda_{De}^2} A_h \approx \frac{1}{4} \frac{n_o e^2}{(m_i T_i)^{1/2}}, \qquad (T_i \approx T_e)$$
$$Y_{he} = 347[mho],$$

where we use Kunkel and Guillory's model[10] for g_{sh}.

* Coupling coefficient

$$\alpha = -2.71,$$
$$\beta = 4.80,$$
$$\gamma = 8.20.$$

Note that the system cannot be driven into instability by the form of the coupling coefficients alone, even if $\alpha < 0$. This can be shown by calculating the total capacitance of the system without L_ϕ, Y_ϕ's and Y_{he}:

$$C_{tot} = C_p + \alpha C_t + \frac{\beta \gamma'}{\beta + \gamma'} C_t > 0,$$

where $\gamma' = (\gamma C_t + C_h)/C_t > \gamma$.

By putting the MFTF-B numerical values for the circuit elements into (21), and solving for the roots of the polynomial with G as a parameter, we obtain Fig.6, the root loci of (21). Note $s = \sigma + j\omega$, with $\sigma < 0$ for stability.

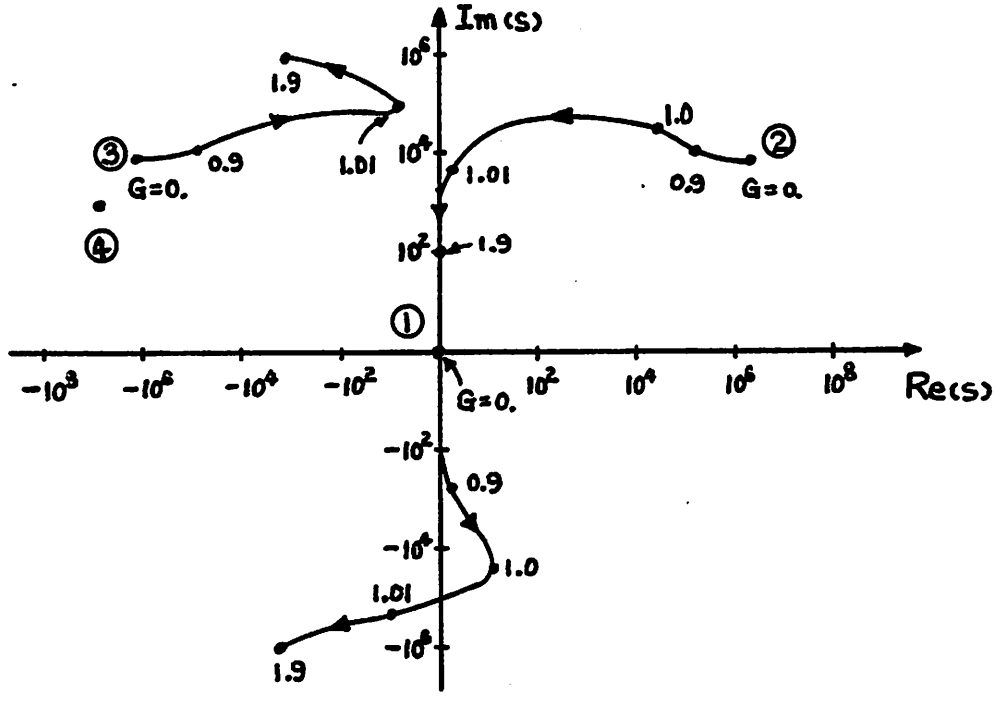

Fig.6 Root loci of the dispersion relation (21) for the MFTF-B.

Without feedback, $G = 0$, we have four roots; root 1 at $(0, 0)$, root 2 at $(1.36 \times 10^6, 9.80 \times 10^3)$, root 3 at $(-1.36 \times 10^6, 9.61 \times 10^3)$, and root 4 at $(-3.37 \times 10^6, 1.12 \times 10^4)$. Root 2 is the flute unstable root that must be stabilized by feedback. Root 3 is the stable conjugate root of 2. The very stable root 4 arises from the $R_{hc}C_{eff}$ time constant of the system, which can easily be seen from the high frequency limit of (21). Root 1 is the zero root of (21) with $G = 0$, which is spurious since it is cancelled out by the pole at zero (root of (23)). However, for $G \neq 0$ the pole - zero cancellation is not exact.

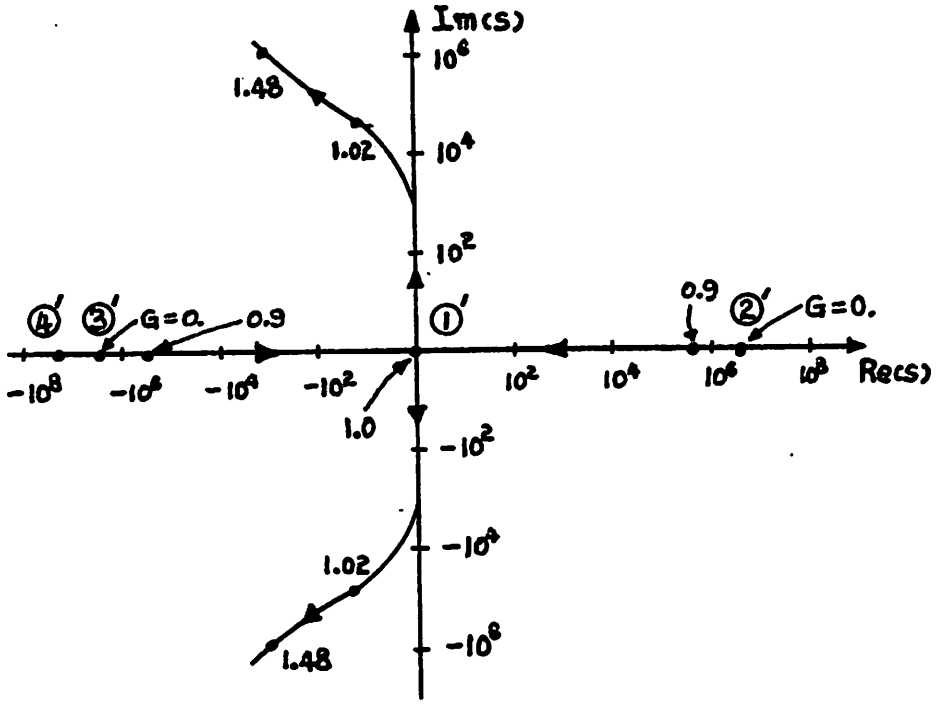

Fig.7 Root loci of the dispersion relation (22) for the MFTF-B.

We can see these interpretations more clearly in Fig.7, which gives the root loci of (22). (All Y_ϕ's are taken to be zero) . Here, for $G = 0$, root 4′ represents the discharging of the total separated charge through the line-tying admittance Y_{he}, root 2′ and 3′ arise from the charge separation due to the gravitational force g, and root 1′ is a spurious root that drops out by the pole - zero cancellation. For $G > 0$, the root loci are continuous with G, except that there is an exchange of stability between roots 1′ and 2′ at $G = 1$. For $G < 1$, root 1′ remains at (0,0); for $G > 1$, root 2′ remains at (0,0). Thus, a spurious root exists at (0,0), for all values of G when the (small) imaginary conductances (Y_ϕ's) are taken to be strictly zero.

In Fig.6, as compared to Fig.7, we introduced a finite $\mathbf{g}_o \times \mathbf{B}_o$ rotational frequency effect through the Y_ϕ's. In this case the pole - zero cancellation is not exact. The effect of rigid rotor motion due to the gravitational force $\mathbf{g}_o$ introduce a time averaging effect on the separated charge, and modifies the effective capacitances. For large enough feedback, i.e., for large enough G, we can see that root 4 remains nearly the same, root 3 remains stable, and roots 1 and 2 exchange their roles. Thus, we send root 2 into the negative half - plane, i.e., we obtain flute stability with large enough feedback, $G > 1$; that is, we convert the flute growing mode into a simple, decaying, rotating mode.

Two interesting limiting cases are $A_t \to 0$, $G \to 0$ i.e., the Irvine model[9], and $R_t \to R_h \gg R_p$. For the case of $A_t \to 0$ and $G \to 0$, applying KCL for Fig.3 we obtain the voltage transfer ratio

$$\begin{aligned}\frac{e_p}{e_h} &= \frac{\beta Y_t}{Y_p + (\alpha+\beta)Y_t} \\ &= \frac{2R_p^2 R_t (R_t^2 + R_h^2)^{1/2} Y_t}{(R_t^2 - R_p^2)^2 Y_p + R_p^2(R_p^2 + R_t^2)Y_t} \\ &\to (1 + \frac{R_h^2}{R_p^2})^{1/2} \qquad as \qquad R_t \to R_p, \qquad i.e., \qquad A_t \to 0\end{aligned} \tag{24}$$

For this case the system can be represented by a transformer - coupled network (Fig.8) with coupling coefficient $n = (1 + (R_h/R_p)^2)^{-1/2}$.

Here, we can see that, if $Y_{he} \to \infty$, the core plasma is shorted out by the perfect line-tying, and the system is stabilized.

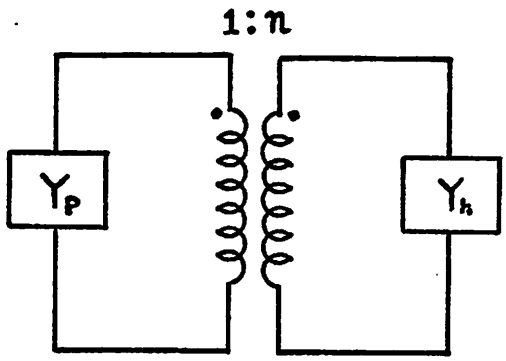

Fig.8 Equivalent circuit representation for A_t, $G \to 0$.

In the other limiting case of $R_t \to R_h \gg R_p$, α, β, γ become

$$\alpha = \frac{R_p^2}{(R_h^2 - R_p^2)^2}((R_p^2 + R_h^2) - 2\sqrt{2}R_h^2),$$

$$\beta = \frac{2\sqrt{2}R_p^2 R_h^2}{(R_h^2 - R_p^2)},$$

$$\gamma = \frac{2R_h^2}{(R_h^2 - R_p^2)}((R_p^2 + R_h^2) - 2\sqrt{2}R_p^2).$$

Then,

$$\alpha Y_t + (\beta Y_t // \gamma Y_t) \to \frac{R_p^2}{R_p^2 + R_h^2} Y_t.$$

For $R_h \gg R_p$, the dispersion relation (18) can be written as

$$\frac{R_p^2}{R_p^2 + R_h^2} Y_t + Y_p = 0.$$

Rewriting the above equation, we obtain

$$\frac{R_p^2}{R_p^2 + R_h^2} \kappa_t R_t^2 + \kappa_p R_p^2 \approx (\kappa_t + \kappa_p) R_p^2 = 0;$$

i.e., $\kappa_t + \kappa_p = 0$, which is physically equivalent to the case of a core plasma surrounded by an infinite external plasma. For $\kappa_t = \kappa_{vac} = 1$, we have a system consisting of a core plasma only.

B. MMX Experiment

We take MMX parameters as follows:

$$B = 1.3[Tesla], \quad l_B = 36cm, \quad R_p = 2cm, \quad \frac{n_t}{n_p} = 0.66,$$
$$n_p = 10^{19}m^{-3}, \quad l_T = 7.5cm, \quad R_t = 3cm, \quad \frac{n_h}{n_p} = 0.11.$$
$$T_p = T_h = T_t = 10[ev], \quad l_p = 7.5cm, \quad R_h = 4cm,$$

The corresponding circuit elements become as follows:

* Capacitors

$$C_p = 2.33 \times 10^{-7}[F],$$
$$C_t = 2.56 \times 10^{-8}[F],$$
$$C_h = 1.54 \times 10^{-7}[F].$$

* Inductor

$$L_p = -1.45 \times 10^{-4}[H].$$

* Frequency-independent part of the imaginary conductance

$$Y_{p\phi} = -j5.54 \times 10^{-5}[mho],$$
$$Y_{t\phi} = -j6.09 \times 10^{-6}[mho],$$
$$Y_{h\phi} = -j3.36 \times 10^{-5}[mho].$$

* Line - tying admittance

$$Y_{he} = 1.80[mho].$$

The root loci plots with and without the Y_ϕ's are given in Fig.s 9 and 10 respectively.

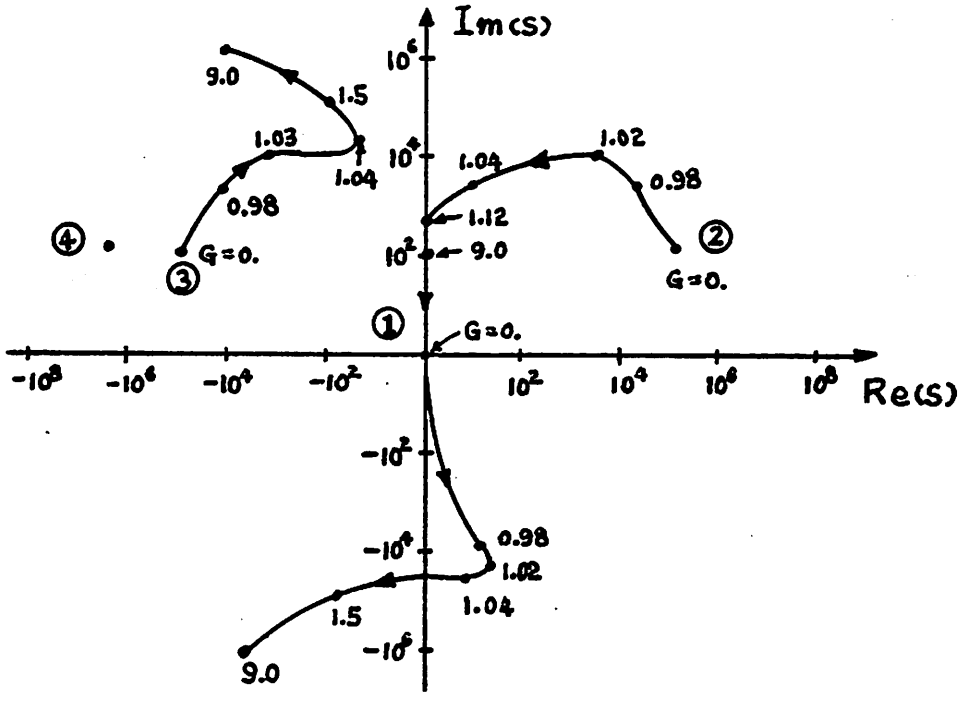

Fig.9 Root loci of the dispersion relation (21) for the MMX.

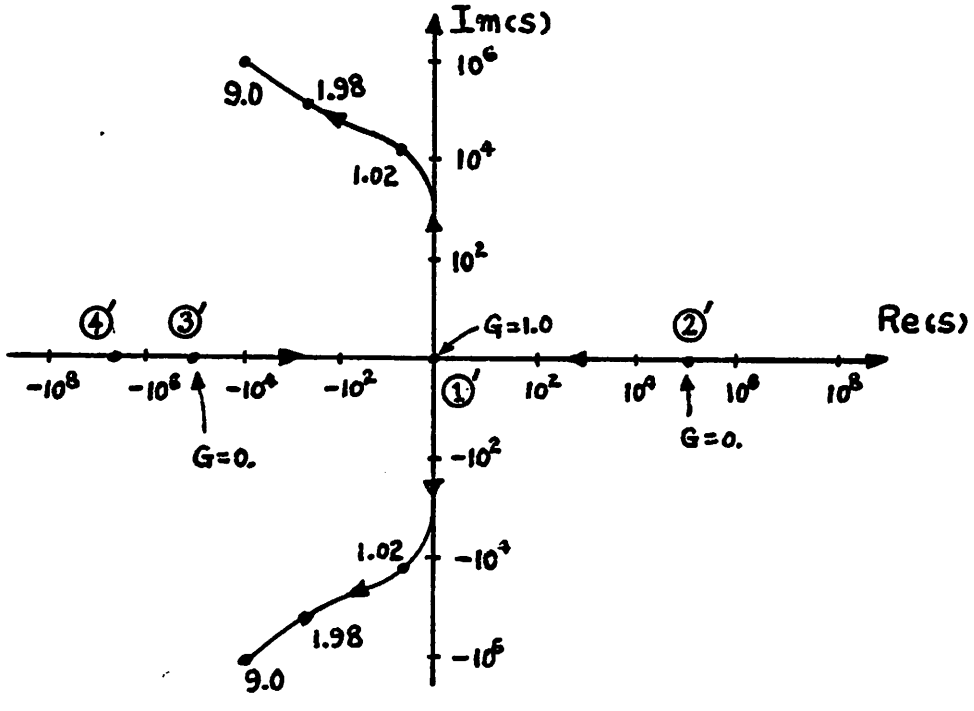

Fig.10 Root loci of the dispersion relation (22) for the MMX.

IV. DISCUSSION AND CONCLUSIONS

The three layer model analysis of axisymmetric mirror machines shows that we can stabilize the $m = 1$ flute unstable core plasma by applying proper feedback signals on segmented, ring-shaped feedback plates which are in contact with the two ends of an external plasma. The feedback signals are applied on the feedback plates through the line-tying admittance of the halo plasma sheath. The constraints on the mode structure change the core - transition plasma boundary conditions to stabilize the core plasma against the flutes. This model ignores finite - β effects, diamagnetic drift effects, and finite Larmor radius effects, and employs sharp boundaries.

The advantage of using active feedback on an end ring in contact with the halo plasma, over modifying the line-tying admittance by employing an emitting end ring, is that the three layer active feedback model predicts that the flute can be suppressed at the core - transition boundary, while the passive model predicts flute stability only if the ring is in contact with a substantial part of the core plasma. Thus, for the active system, by a proper choice of feedback transfer function, we can obtain absolute stability with sufficiently large inner radius of the feedback plates that the plasma end loss heat flux and the radiation or neutron damage on the feedback plates can be held to acceptable levels.

* This work was supported by Department of Energy Contract DE-AT0E 76ET53059. Helpful discussion with A. J. Lichtenberg are greatefully acklowledged.

Appendix

The physical meaning of the circuit elements LCR of the plasma can be seen from the guiding center approximation for the $m = 1$ mode:

i) Polarization drift

$$\begin{aligned}
\mathbf{v}_s &= \frac{m_s}{e_s B^2}\frac{d\mathbf{E}}{dt} \\
&= \frac{m_s \omega \mathbf{k}\phi}{e_s B^2} \\
J_{pol} &= \sum_s \omega \frac{m_s n_o l_T}{B^2} k\phi \\
&= \omega \sum_s \frac{m_s n_o l_T}{B^2 R_p}\phi \\
&\equiv \omega C_p' \phi
\end{aligned}$$

where $C_p' = C_p/\pi R_p$ is the core capacitance per unit arc length of the core boundary.

ii) First order $\mathbf{g} \times \mathbf{B}$ drift

$$\mathbf{v}_s = \frac{m_s}{e_s}\frac{\mathbf{g}_1 \times \mathbf{B}}{B^2}$$

using $g_1 \approx \xi v_{th}^2 l_p / l_B^2 l_T$, and $\xi \approx k\phi/\omega B$ for the low-β, near-axis plasma, we have

$$\begin{aligned}
J_{grav.} &\approx \sum_s \frac{n_o m_s g_{1s}}{B} \\
&= \sum_s \frac{n_o m_s v_{ths}^2}{B l_B^2} l_p \xi \\
&= \frac{1}{\omega}\sum_s \frac{n_o m_s v_{ths}^2 l_p}{B^2 R_p l_B^2}\phi \\
&\equiv \frac{1}{\omega L_p'}\phi
\end{aligned}$$

where $L'_p = L_p/(\pi R_p)$ is the core inductance pre unit arc length of the core boundary.

iii) Finite rotational frequency effect correction

$$Y_{p\phi} = -jC_p 2\bar{\epsilon}\Omega_i$$
$$= jC_p k v_{go}$$

where, v_{go} is the zeroth order $\mathbf{g} \times \mathbf{B}$ drift velocity. If we rewrite the admittance of the capacitor to include $Y_{p\phi}$, we have

$$Y_c = j\omega C_p(1 + \frac{kv_{go}}{\omega}).$$

This is the finite rotational frequency corrected admittance of the core capacitor. This effect slightly reduces the flute growth rate.

References

[1]Lieberman, M. A. and Wong, S. L., *Plasma Physics* **19** 745 (1977)

[2]Wong, S. L. and Lieberman, M. A., *Plasma Physics* **20** 403 (1977)

[3]Wong, S. L., Ph.D. Thesis, University of California, Berkeley (1978)

[4]Vandegrift, G. G., Ph.D. Thesis, University of California, Berkeley (1982)

[5]Moir, R. (ed.), Lawrence Livermore Laboratory Report UCID-16736 (1975)

[6]Chuyanov, V. A., Culham Laboratory Report CTO/598 (1969)

[7]Wickham, M. and Vandegrift, G. G., *Physics of Fluids* **25** 52 (1982)

[8]Vandegrift, G. G. and Timothy, G., Technical Report 83-71, Department of Physics, University of California, Irvine (1983)

[9]Vandegrift, G. G., Good, T. N., and Rynn, N., *Bull. Am. Phys Soc.* **28** 1048 (1983)

[10]Kunkel, W. K. and Guillory, J., *7th International Conference on Phenomena in Ionized Gases* Vol.2, Perovic, B. and Tosic, D. (ed.), Belgrade (1965)